CSIRO PUBLISHING

Functional Plant Biology, 2017, **44**, 302–311
http://dx.doi.org/10.1071/FP16214

Photoprotective and antioxidative mechanisms against oxidative damage in *Fargesia rufa* subjected to drought and salinity

Cheng-Gang Liu[A,E], *Qing-Wei Wang*[B], *Yan-Qiang Jin*[C], *Kai-Wen Pan*[C] *and Yan-Jie Wang*[C,D,E]

[A]Key Laboratory of Tropical Plant Resources and Sustainable Use, Xishuangbanna Tropical Botanical Garden, Chinese Academy of Sciences, Menglun, 666 303, China.
[B]Graduate School of Life Sciences, Tohoku University, Aoba, Sendai, 980-8578, Japan.
[C]Chengdu Institute of Biology, Chinese Academy of Sciences, Chengdu, 610 041, China.
[D]College of Life Science, Sichuan Normal University, Chengdu, 610 101, China.
[E]Corresponding authors. Emails: chengangliu@hotmail.com; wyjilwm2015@163.com

Abstract. Drought and salinity are the two most common and frequently co-occurring abiotic stresses limiting plant productivity worldwide, yet it remains unclear whether bamboo species possess effective mechanisms to protect against oxidative damage caused by drought and salinity, either alone or in combination. In this study, we utilised *Fargesia rufa* Yi, a species important to forest carbon sequestration and endangered giant pandas, to evaluate physiological, biochemical and ultrastructural responses to drought, salinity and their combination. Under drought alone, *F. rufa* exhibited reduced water loss from leaves, photochemistry inhibition, pigment degradation, reactive oxygen species accumulation, lipid peroxidation, and damage to organelles compared with salinity and combined stress treatments. The superior performance under drought alone was attributed to greater thermal dissipation and the water-water cycle capacities, increased SOD/AsA-GSH cycle enzymes activities, and a favourable redox balance of antioxidants. Therefore, relative to salinity alone and drought + salinity, *F. rufa* plants under drought exhibit highly efficient mechanisms to protect against oxidative damage, which most likely allow accelerated recovery of photosynthetic plasticity once the stress is removed.

Additional keywords: antioxidative enzymes, bamboo, drought, electron transport, leaf ultrastructure, salt stress.

Received 13 June 2016, accepted 8 November 2016, published online 5 January 2017

Introduction

Drought and salinity are two serious and frequently co-occurring abiotic stresses that dramatically constrain plant growth and yield (Ahmed *et al*. 2015). It is currently estimated that approximately one third of the world's arable land experiences cyclical or unpredictable drought (Chaves and Oliveira 2004), and more than 800 million hectares of land are subjected to salinity (Munns 2005). Furthermore, these abiotic stresses are becoming increasingly widespread and severe due to climate change and increased competition for land, water and energy (Morari *et al*. 2015). At tissue and cellular levels, plants typically show similar responses to isolated drought or salinity stress, such as slow growth, loss of cell plasticity, ionic imbalance, decreased photochemical activity, accumulation of osmoprotectants, upregulation of antioxidative enzymes, changes in phytohormones and overexpression of genes (Filippou *et al*. 2014; Muscolo *et al*. 2015; Razzaghi *et al*. 2015). However, these common responses are influenced by the intensity and duration of the stress as well as the plant species (Chaves *et al*. 2009). Moreover, stress often occurs in combination, for example, drought and salinity (Chen *et al*. 2010; Ahmed *et al*. 2015; Dawalibi *et al*. 2015), and recent studies indicate that plant physiological, biochemical and molecular responses to the combination of drought and salinity are unique and cannot be directly deduced from each stress applied individually (Suzuki *et al*. 2014). Therefore, a complete understanding of interactions between these stresses is of great ecological significance and is important for developing sustainable plant productivity strategies.

Bamboos species with a woody vascular bundle structure are an important component of many forest ecosystems, accounting for ~13% of Gramineae genera (87 of 660) and nearly 15% of Gramineae species (1500 of 10 000). These species are unevenly distributed in tropical, subtropical and temperate regions of the world (31.5 million ha in total), and despite strong decreases in the area of total forest in most countries, regions of bamboo forest are progressively increasing (Scurlock *et al*. 2000). China has long been known as the 'Kingdom of bamboo' in terms of the number of species (>500 species in 39 genera) and area (6.7 million ha), and as a renewable resource, bamboo can provide economic and ecological benefits for humans. Nonetheless, the growth characteristics of bamboo, e.g. relatively fast growth, high production and rapid maturity from shoot to culm, differ from those of woody and herbaceous plants (Yen *et al*. 2010). Moreover, owing to their unusual extended sexual reproduction interval and limited seed dispersal ability, several

bamboo species are extremely vulnerable to a changing environment (Tuanmu *et al*. 2013). Although previous studies have intensively focussed on species-specific morphological responses to isolated stresses, few data are available regarding ecological and physiological processes of bamboo species in response to combined stress.

Fargesia rufa Yi, which grows in the understory of subalpine dark coniferous forest and hinders tree seedlings regeneration, especially species that prefer to establish on the forest floor (Li *et al*. 2013), is one of the bamboo species that is a staple food of endangered giant pandas. However, due to its shallow roots, *F. rufa* is highly susceptible to water deficit (Liu *et al*. 2015*a*), which causes leaf loss, early flowering and even death, thus resulting in a potential shortage of food for endangered pandas (Tuanmu *et al*. 2013). To avoid the adverse abiotic conditions of their habitats, *ex situ* conservation of giant pandas has been actively carried out in China and abroad, and as a consequence, transplantation of bamboo is necessary, with utilisation of poor quality land such as saline-alkali soil. Our recent studies demonstrated that *F. rufa* can acclimate to variable water regimes through differential regulation of carbon and nitrogen metabolism (i.e. osmotic adjustment) and that phosphorus application can further alleviate damage due to soil water deficit (Liu *et al*. 2015*a*, 2015*b*). Nonetheless, little is known about the photoprotective and antioxidative processes of *F. rufa* that protect against oxidative damage caused by isolated and combined drought and salinity stresses.

In the present study, leaf ultrastructure, photosynthesis, light-energy partitioning, antioxidative capacity and lipid peroxidation were investigated in *F. rufa* plants subjected to isolated and combined drought and salinity treatments. The objectives were to determine whether *F. rufa* possesses efficient mechanisms to protect against photochemical damage and oxidative stress induced by drought and salinity and, if so, whether the same processes are invoked under different stress conditions. The results of this study will contribute to the comprehensive understanding and exploration of stress-tolerant bamboo species.

Materials and methods

Plant materials and experimental design

Two-year-old *F. Rufa* Yi plants were collected from the permanent nursery at Wanglang National Nature Reserve (31°42′N, 103°54′E) in Sichuan Province, China in March 2013. The mean elevation and annual rainfall in this area are 2590 m and 860 mm respectively. The plants were transplanted into 50 L plastic pots filled with 30 kg homogenised soil (pH = 6.75 ± 0.14), which consisted of sieved surface soil (0–30 cm) from the experimental site. The plants were grown during the treatment period under ambient conditions of daytime temperature of 13–33°C, a night-time temperature of 8–15°C and RH of 40–85% in a naturally lit greenhouse that provided shelter from rainfall at Maoxian Mountain Ecosystem Research Station, Chinese Academy of Sciences. Before initiation of the experiment, all pots were kept moist by regular watering every 2 days. The treatment started ~5 months after transplanting and was applied for a month (i.e. from 15 August to 16 September 2013).

The experiment was a completely randomised design with four factorial combinations of two levels of drought and salinity. Plants were irrigated daily with a Hoagland's nutrient solution for 1 week before starting the treatments. Eighty uniform and healthy plants were chosen for the different treatments (four replications, five plants in each replication). The plants divided into two groups: one group was watered with a nutrient solution containing 20 mM NaCl for the first 5 days (200 mL every day, 1 L in total), and another watered with the same nutrient solution lacking salt. The plants of each of the above treatments were further divided into two groups, either subjected to drought stress (30% field capacity, FC) or not (80% FC) for a month. Therefore, the experiment consisted of four treatments: control (80% FC + 0 mM NaCl), drought (30% FC + 0 mM NaCl), salinity (80% FC + 20 mM NaCl) and drought + salinity (30% FC + 20 mM NaCl). The pots were weighed every day and rewatered to 30 and 80% FC (i.e. soil water contents of 10.9 and 26.4% respectively) by replacing the amount of transpired water. To avoid systematic error due to possible differences in fluctuating environmental conditions, all pots were rotated every 5 days during the experiment. The newly developed and sun-oriented leaves were sampled at 0900 hours at the end of experiment and immediately stored at –80°C for further analyses.

Determination of leaf water status

The leaf relative water contents (RWC) was calculated as follows: RWC (%) = (FW – DW)/(TW – DW) × 100, where FW is the fresh weight, TW is the turgid weight after soaking in deionised water for 12 h, and DW is the dry weight after drying at 70°C for 48 h.

Measurement of gas exchange and chlorophyll fluorescence

On the day before sampling, leaf gas exchange and chlorophyll fluorescence were measured simultaneously using a LI-6400 portable infrared gas exchange analyser equipped with a fluorometer attachment (LI-COR Biosciences). The net photosynthetic rate (P_n), stomatal conductance (g_s), intercellular CO_2 concentration (C_i), light-adapted maximum (F_m'), minimum (F_0') and steady-state (F_s) fluorescence yield were determined at 0900 hours. After determination of light-adapted parameters, the plants were fully covered with black opaque plastic bags and maintained for 40 min. A saturating pulse (8000 μmol m^{-2} s^{-1}) was then applied over 0.8 s, and the maximum photochemical efficiency of PSII (F_v/F_m) was recorded.

Estimation of absorbed light energy by PSII

The light energy absorbed by PSII is consumed by three competitive pathways: (i) ΔpH- and xanthophyll-regulated thermal dissipation (Φ_{NPQ}, $F_s/F_m' - F_s/F_m$); (ii) fluorescence and constitutive thermal dissipation ($\Phi_{f,D}$, F_s/F_m); and (iii) apparent electron transport (Φ_{PSII}, $1 - F_s/F_m'$), where $\Phi_{NPQ} + \Phi_{f,D} + \Phi_{PSII} = 1$. The rate of energy dissipation via each process (J_{NPQ}, $J_{f,D}$, J_{PSII}) was calculated by multiplying the respective quantum efficiency by the assumed proportion of absorbed quanta used by PSII reaction centres, irradiance and leaf absorption, respectively (Hendrickson *et al*. 2004). Moreover, the rates of carboxylation (V_c) and oxygenation (V_o)

by RuBP were estimated as described by Miyake and Yokota (2000). The electron fluxes in the two cycles (photosynthetic carbon reduction and photorespiratory carbon oxidation) can be expressed as $J_c = 4 \times V_c$ and $J_o = 4 \times V_o$ respectively. An alternative electron flux (J_a) not used in the above two cycles can be estimated from the equation $J_{PSII} - (J_c + J_o)$.

Determination of photosynthetic pigments

Xanthophyll cycle pigments (A, antheraxanthin; L, lutein; V, violaxanthin; Z, zeaxanthin) in frozen leaves were extracted in the dark using 80% acetone, filtered through a 0.45 µm membrane and analysed by reversed-phase high-performance liquid chromatography (HPLC) (Prominence UFLC, Shimadzu) (Thayer and Björkman 1990). A Spherisorb C18 column (5 µm, Φ4 × 250 mm) was used at a flow rate of 1.5 mL min^{-1}. Pigments were eluted using 100% solvent A (acetonitrile/methanol, 75 : 25) for the first 7 min followed by a 2 min linear gradient to 100% solvent B (methanol/ethyl acetate, 70 : 30), which continued isocratically until the end of the 30 min separation. Before the next injection, the column was allowed to re-equilibrate for 10 min in solvent A. Pigments in 10 µL of extract injected were detected by their absorbance at 445 nm. The de-epoxidation state for the xanthophyll cycle was expressed as (A + Z)/(V + A + Z). Quantification of chlorophylls (Chl *a* + *b*) and carotenoids (Car) via spectrophotometric absorbance at 470, 645 and 662 nm was conducted.

Measurement of reactive oxygen species (O_2•$^-$ and H_2O_2) and lipid peroxidation

The rate of O_2•$^-$ production was measured by monitoring nitrite formation from hydroxylamine. Briefly, frozen leaves were homogenised in 65 mM sodium phosphate buffer (SPB, pH 7.8) and centrifuged at 5000*g* for 10 min. After incubation of a mixture containing 65 mM SPB (pH 7.8), 10 mM hydroxylammonium chloride and supernatant for 20 min at 25°C, 17 mM sulfanilamide and 7 mM α-naphthylamine were added. Ethyl ether in the same volume was then added, and the sample was centrifuged at 1500*g* for 5 min. The absorbance of the aqueous solution at 530 nm was determined. The H_2O_2 content was measured by monitoring the titanium-peroxide complex. Frozen leaves were homogenised in acetone and centrifuged at 3000*g* for 10 min. A mixture containing 20% titanium tetrachloride in concentrated HCl, ammonia and supernatant was centrifuged at 3000*g* for 10 min. The resulting precipitate was washed five times with ice-cold acetone and solubilised with 1 M H_2SO_4, and the absorbance at 410 nm was measured. Lipid peroxidation was estimated by monitoring malondialdehyde (MDA) according to the thiobarbituric acid (TBA) test. Frozen leaves were homogenised in 50 mM SPB (pH 7.8) and centrifuged at 12 000*g* for 20 min. Supernatant (1 mL) was mixed with 20% trichloroacetic acid (TCA) containing 2% TBA. The mixture was heated in boiling water for 30 min and quickly cooled in an ice bath. After centrifugation at 15 000*g* for 10 min, the absorbance of the supernatant at 532 and 600 nm was measured. The amount of MDA was calculated based on an extinction coefficient of 155 mM^{-1} cm^{-1}.

Determination of antioxidative enzymes activities and antioxidant contents

For analysis of antioxidative enzymes activities, frozen leaves were extracted with 2 mL of 50 mM SPB (pH 7.8) containing 0.2 mM EDTA, 2% polyvinylpyrrolidone and 2 mM reduced ascorbate (AsA). The extract was centrifuged at 12 000*g* for 20 min, and the supernatant was used for the enzyme analysis. All procedures were performed at 4°C. Superoxide dismutase (SOD) activity was measured using a previously described photochemical method (Giannopolitis and Ries 1977). The reaction contained supernatant and nitroblue tetrazolium (NBT) solution, including 50 mM SPB (pH 7.8), 0.1 mM EDTA, 63 µM NBT, 13 mM methionine, and 1.3 µM riboflavin. One unit of SOD activity was defined as the amount of enzyme required to cause a 50% inhibition in the rate of *p*-nitro blue tetrazolium chloride reduction at 560 nm. Catalase (CAT) activity was measured in a reaction containing 25 mM SPB (pH 7.0), 10 mM H_2O_2 and supernatant (Cakmak and Marschner 1992), as detected at 240 nm ($E = 39.40$ mM^{-1} cm^{-1}). Ascorbate peroxidase (APX) activity was measured in a reaction containing 25 mM SPB (pH 7.0), 0.1 mM EDTA, 5 mM AsA, 20 mM H_2O_2 and supernatant (Nakano and Asada 1981), as detected at 290 nm ($E = 2.88$ mM^{-1} cm^{-1}). Glutathione reductase (GR) activity was determined in a reaction containing 25 mM SPB (pH 7.8), 2.4 mM NADPH, 10 mM oxidised glutathione (GSSG) and supernatant (Foyer and Halliwell 1976), as detected at 340 nm ($E = 6.22$ mM^{-1} cm^{-1}). Monodehydroascorbate reductase (MDHAR) activity was measured in a reaction containing 25 mM SPB (pH 7.8), 0.2 mM of EDTA, 0.1 mM AsA, 0.5 U AsA oxidase, 4 mM NADH and supernatant (Arrigoni *et al*. 1981), as detected at 340 nm ($E = 6.22$ mM^{-1} cm^{-1}). Dehydroascorbate reductase (DHAR) activity was assayed in a reaction containing 25 mM SPB (pH 7.0), 0.1 mM EDTA, 8 mM DHA, 70 mM reduced glutathione (GSH) and supernatant (Foyer and Halliwell 1976), as detected at 265 nm ($E = 14.6$ mM^{-1} cm^{-1}). All reactions proceeded at 25°C in 2-mL quartz cuvettes. Data are expressed as specific activity, with the protein content determined using the Bradford method.

For examination of ascorbate and glutathione contents, frozen leaves were extracted with 5% TCA and assessed using a described method (Arrigoni *et al*. 1981). The reaction for total ascorbate contained 150 mM SPB with 5 mM EDTA (pH 7.4), 10 mM dithiothreitol (DTT) and supernatant. After incubation for 10 min at 25°C, 0.5% N-ethylmaleimide was added to remove excess DTT. The AsA content was determined in a similar reaction mixture, except that deionised H_2O was added instead of DTT and N-ethylmaleimide. Colour developed in the mixtures after addition of 10% TCA, 44% orthophosphoric acid, 4% 2, 2′-bipyridyl and 3% $FeCl_3$. The mixtures were incubated at 40°C for 40 min, and absorbance at 525 nm was quantified. The DHA content was estimated from the difference between total ascorbate and AsA. The total glutathione and GSSG contents were measured using the 5,5′-dithiobis-2-nitrobenzoic acid (DTNB)–GR recycling procedure. Total glutathione was assayed spectrophotometrically at 412 nm at 25°C, using 0.1 U baker's yeast GR, 6 mM DTNB and 2 mM NADPH. GSSG was evaluated in a similar manner after removal of GSH via 2-vinylpyridine derivatisations. GSH was estimated from the difference between total glutathione and GSSG.

Ultrastructural observations of mesophyll cells

Transmission electron microscopy (TEM) was performed on small sections (1–2 mm in length) of sun-oriented leaves. Leaflets were fixed in 3% glutaraldehyde in 0.1 M SPB (pH 7.2) for 8 h at 4°C, post-fixed in 1% osmium tetroxide for 2 h and immersed in 0.1 M phosphate buffer for 2 h. The material was then dehydrated through a graded ethanol series (50, 60, 70, 80, 90, 100%, 20 min each step) and embedded in Epon 812. Ultrathin sections (80 nm) were cut using an ultramicrotome (Reichert-Jung Ultracut E), stained with uranylacetate and lead citrate and mounted onto copper grids for viewing in the H-600IV TEM (Hitachi).

Statistical analysis

All analyses were performed with the SPSS software package 17.0 (SPSS Inc.). Data were subjected to ANOVA, and the mean values of four replicates were compared using Duncan's test at a significance level of $P < 0.05$. Before ANOVA, the data were checked for normality and homogeneity of variance and when needed, log-transformed to correct deviations from these assumptions.

Results

Effects of drought and salinity on water status, photosynthetic performance and pigment composition

In this study, *F. rufa* plants were subjected to isolated and combined stresses of drought and salinity. RWC, a good indicator of the leaf hydration status, decreased significantly under all stress treatments compared with the control, with the largest decline (by 34.3%) under combined stress (Fig. 1*a*). The P_n, g_s, F_v/F_m also decreased obviously, especially under salinity and combined stress, whereas NPQ was enhanced by 119.2 and 169.2% respectively (Fig. 1*b*, *c*, *e*, *f*). There was no significant difference in P_n and C_i between salinity and combined stress (Fig. 1*b*, *d*).

In comparison with the control, the contents of photosynthetic pigments, including Chl *a* + *b* and Car, decreased markedly under stress treatments, but no differences in these parameters were observed between salinity and combined stress (Table 1). The total xanthophyll cycle pigment (V + A + Z) content also notably declined under stress, whereas L content exhibited an increase. Conversely, the de-epoxidation state of the xanthophyll cycle ((A + Z)/(V + A + Z)) increased appreciably, especially

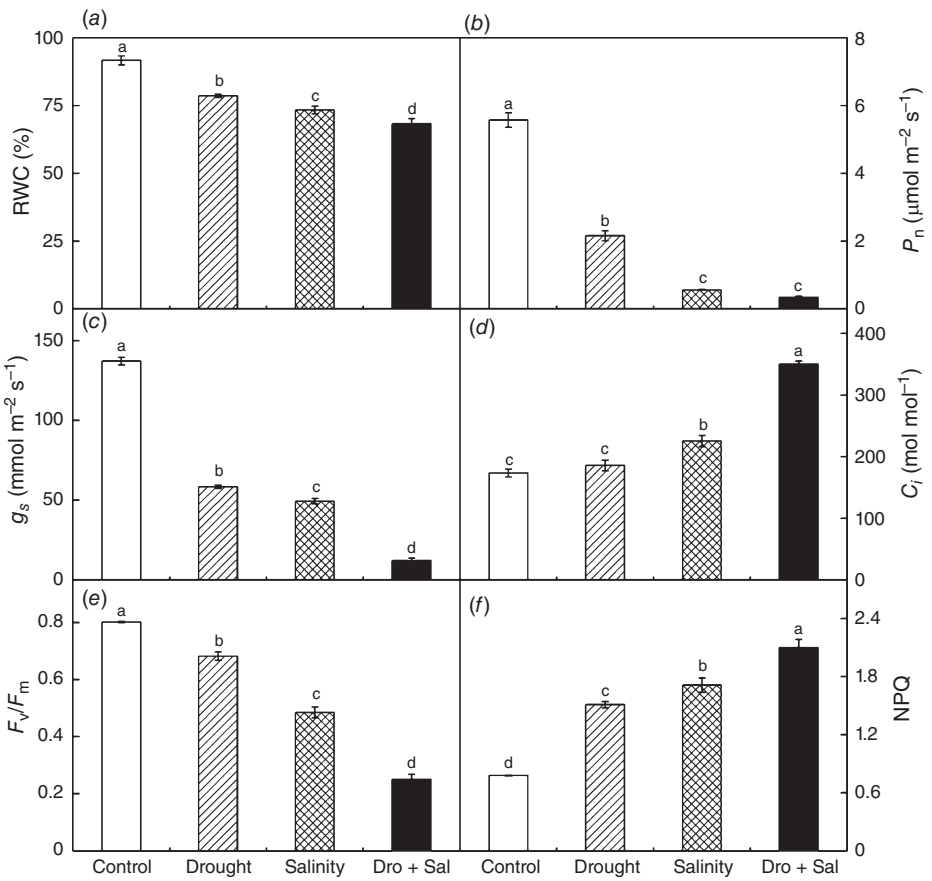

Fig. 1. Leaf water status and photochemical characteristics of *Fargesia rufa* plants subjected to drought, salinity and their combination. (*a*) Relative water content (RWC) of leaves; (*b*) net photosynthetic rate (P_n); (*c*) stomatal conductance (g_s); (*d*) intercellular CO_2 concentration (C_i); (*e*) maximum photochemical efficiency of PSII (F_v/F_m); (*f*) non-photochemical quenching (NPQ). Data are the means of four replicates with s.e. shown by vertical bars. Different letters indicate a significant difference at the 5% level.

under salinity and combined stress, at 116.7 and 141.7%, respectively, higher than that of the control.

Effects of drought and salinity on electron flux allocation

Under drought, salinity and combined stress, J_{NPQ} increased by 52.1, 70.1 and 92.3%, whereas $J_{f,D}$ decreased by 21.8, 22.5 and 28.5%, respectively, in comparison with the control (Table 2). There was no significant difference in J_{NPQ} and $J_{f,D}$ between drought and salinity, but a significant reduction in J_{PSII} was detected after stress treatments. Compared with the control, the proportion of J_{NPQ} to total energy under stress was substantially increased by 18–31%, though the proportions of $J_{f,D}$ and J_{PSII} to total energy decreased by 10–13% and 8–18% respectively. J_{PSII} comprises J_c, J_o and J_a, and compared with the control, J_c and J_o declined markedly under stress, especially salinity and combined stress. In contrast, J_a increased by 50.0 and 12.5% under drought and salinity, respectively, but was strongly inhibited by 68.8% under combined stress. Under stress, the proportions of J_c and J_o to J_{PSII} decreased by 24–28% and 11–18%, whereas the proportion of J_a to J_{PSII} increased by 34–46%.

Effects of drought and salinity on leaf ultrastructure

Although some plastoglobuli were found in mesophyll cell organelles under drought, the cells essentially appeared normal in leaves from control and drought-treated *F. rufa* plants (Fig. 2). However, under salinity and combined stress it was observed that (i) the structures of chloroplast and mitochondria were badly damaged with numerous plastoglobuli; (ii) the thylakoid network was visibly incomplete, and the number of grana decreased as a result of thylakoid membranes degradation; and (iii) the mitochondrial shape became swollen, and their inner membranes were severely degraded.

Effects of drought and salinity on radical-scavenging system

Compared with the control, the levels of $O_2^{\bullet -}$ and H_2O_2 increased notably under stress (Fig. 3*a*, *b*), and MDA levels increased by 105.4, 123.7 and 167.3% under drought, salinity and combined stress respectively (Fig. 3*c*). However, no significant difference in MDA content was observed between drought and salinity or between salinity and combined stress.

Antioxidative enzymes, such as SOD, CAT, APX, MDHAR, DHAR and GR, showed different response patterns to drought, salinity and combined stress (Fig. 4). Compared with the control, similar increases (~16.0%) in SOD activity were observed among the treatments (Fig. 4*a*). CAT activity was stimulated by 101.5 and 131.0% under salinity and combined stress, respectively, but was not affected by drought alone (Fig. 4*b*). Activities of APX and DHAR increased significantly under stress, in particular, by 134.6 and 56.1% under drought and combined stress respectively (Fig. 4*c*, *e*). Enhancement of MDHAR and GR activities were observed only under drought, by 112.5 and 60.6%, but the values in the other stress treatments were similar to that of the control (Fig. 4*d*, *f*).

The contents of total ascorbate (AsA + DHA) and glutathione (GSH + GSSG) increased substantially under stress compared with the control (Fig. 5): 30.0 and 45.7% and 27.4 and 24.6% higher under salinity and combined stress, respectively, than in the control. The AsA/DHA ratio did not alter under drought, but it was inhibited by 40.2 and 44.2% under salinity and combined stress, respectively, in comparison with the control (Fig. 5*a*). The GSH/GSSG ratio under drought was similar to that of the

Table 1. Pigments of *Fargesia rufa* plants subjected to drought, salinity and their combination

Data are the mean ± s.e. ($n = 4$). Values followed by different letters indicate a significant difference at the 5% level. Abbreviations: Chl $a + b$, chlorophyll $a + b$; Car, carotenoids; A, antheraxanthin; V, violaxanthin; Z, zeaxanthin; L, lutein

Treatment	Chl $a + b$ (mg g^{-1} FW)	Car (mg g^{-1} FW)	V + A + Z (mmol mol^{-1} Chl)	(A + Z)/(V + A + Z)	L (mmol mol^{-1} Chl)
Control	2.61 ± 0.06a	0.62 ± 0.01a	61.20 ± 0.60a	0.24 ± 0.01d	183.88 ± 0.69b
Drought	1.82 ± 0.05b	0.54 ± 0.01b	54.46 ± 0.94b	0.30 ± 0.01c	201.73 ± 2.96a
Salinity	0.89 ± 0.07c	0.34 ± 0.02c	45.30 ± 2.65c	0.52 ± 0.01b	206.73 ± 3.20a
Drought + salinity	0.87 ± 0.04c	0.31 ± 0.01c	28.88 ± 1.44d	0.58 ± 0.01a	198.76 ± 8.23ab

Table 2. Energy flux of *Fargesia rufa* plants subjected to drought, salinity and their combination

Data are the mean ± s.e. ($n = 4$). Values followed by different letters indicate a significant difference at the 5% level. Abbreviations: J_{NPQ}, energy flux via ΔpH- and xanthophyll-regulated thermal dissipation; $J_{f,D}$, energy flux via fluorescence and constitutive thermal dissipation; J_{PSII}, electron transport rate at PSII; J_c, electron transport for photosynthetic carbon reduction; J_o, electron transport for photorespiratory carbon oxidation; J_a, alternative electron transport

Treatment	Energy flux (μmol $e^- m^{-2} s^{-1}$)					
	J_{NPQ}	$J_{f,D}$	J_{PSII}	J_c	J_o	J_a
Control	117 ± 6c	151 ± 10a	69 ± 2a	37 ± 6a	16 ± 3a	16 ± 2b
Drought	178 ± 4b	118 ± 7b	42 ± 4b	13 ± 2b	5 ± 1b	24 ± 2a
Salinity	199 ± 5b	117 ± 4b	23 ± 3c	3 ± 1c	2 ± 0c	18 ± 3ab
Drought + salinity	225 ± 8a	108 ± 3c	7 ± 1d	2 ± 0c	1 ± 0c	5 ± 1c

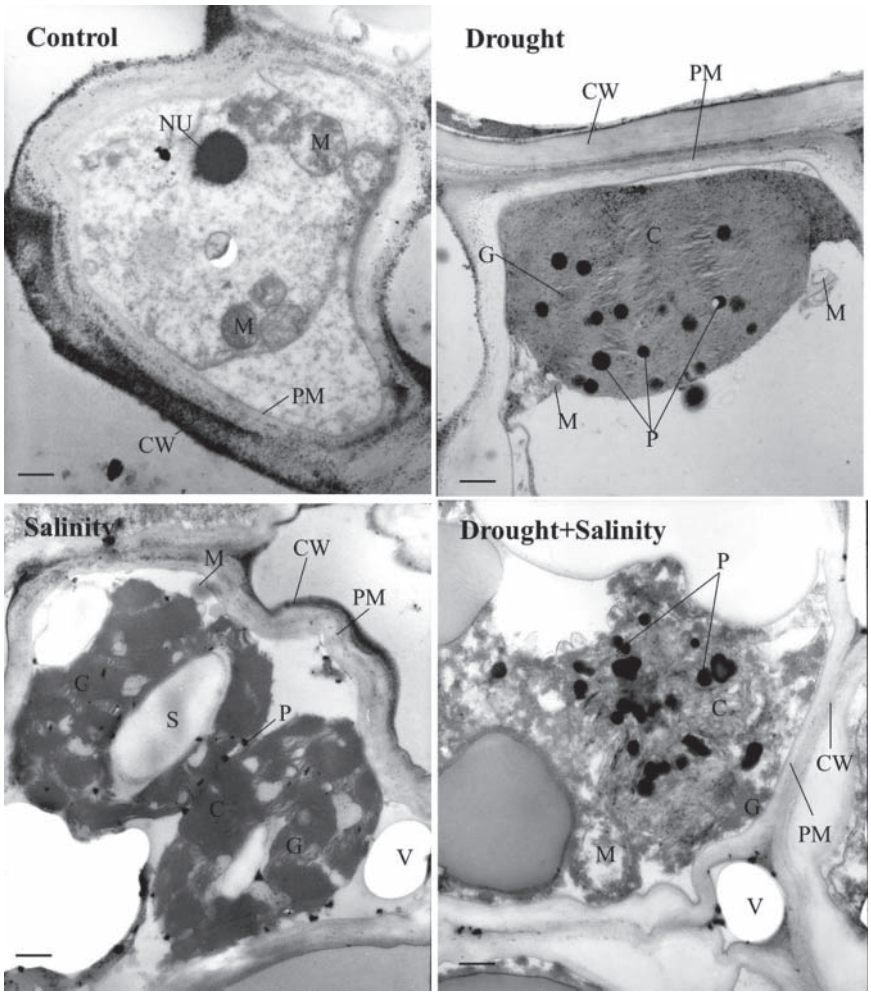

Fig. 2. Transmission electron microscopy observations of mesophyll cells of *Fargesia rufa* plants under control and stress conditions. The bars shown are 0.5 µm. Abbreviations: C, chloroplast; CW, cell wall; G, granum; M, mitochondria; N, nucleus; P, plastoglobulus; PM, plasma membrane; S, starch granule; V, vacuole.

control, but it was increased by 90.2 and 51.1% under salinity and combined stress respectively (Fig. 5*b*).

Discussion

Photosynthesis is extremely sensitive to any changes in environmental conditions such as drought and salinity, which involves the interplay of limitations taking place at different sites of the cell and at different times in relation to plant development (Chaves *et al*. 2009). Nonetheless, it remains controversial whether drought inhibits CO_2 assimilation through stomatal or nonstomatal factors. In this study, *F. rufa* plants displayed sharp decreases in P_n in parallel with RWC, PSII activity (F_v/F_m), and pigment degradation (Chl *a* + *b* and Car) under drought, especially under salinity and combined stress (Fig. 1; Table 1). Furthermore, an increase in C_i accompanied by g_s was observed under all stresses. These results indicate that photosynthetic inhibition can largely be attributed to both diffusive resistance and metabolic impairment. In addition, some studies have reported that photosynthetic capacity could not recover in many C_3 plants when P_n was reduced by >80% and/or when g_s dropped below 0.1–0.05 mol H_2O m^{-2} s^{-1} (Flexas *et al*. 2006). Based on this evidence, we speculated that *F. rufa* photosynthetic activity might be restored only under drought due to the relatively higher P_n, g_s and normal mesophyll cell organelles (Fig. 2). These findings suggest an acclimatory response of the photosynthetic apparatus, especially PSII, to drought but not to salinity and combined stress.

As changes in photosynthetic capacity are closely associated with alterations in light energy absorption and allocation, quantification of the fate of energy absorbed by PSII antennae after stress is important for elucidating the photoprotective mechanism involved in acclimation (Hendrickson *et al*. 2004). Although they are competitive in general, an explicit trade-off exists among the three fates of energy: J_{NPQ}, $J_{f,D}$ and J_{PSII} (Chen *et al*. 2016). Among the three pathways, we found that in *F. rufa*, J_{NPQ} markedly increased to compensate for inferior photosynthetic capacity, as revealed by reductions in J_{PSII}

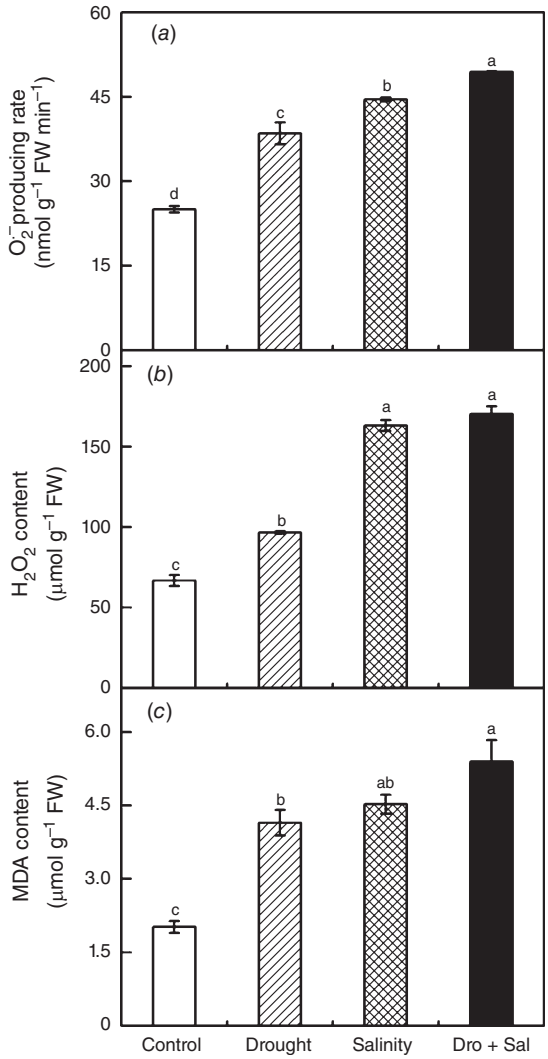

Fig. 3. Reactive oxygen species and lipid peroxidation in *Fargesia rufa* plants subjected to drought, salinity and their combination. (*a*) Superoxide anion ($O_2^{\bullet-}$); (*b*) hydrogen peroxide (H_2O_2); (*c*) malondialdehyde (MDA). Data are the means of four replicates with s.e. shown by vertical bars. Different letters indicate a significant difference at the 5% level.

and $J_{f,D}$ after drought and salinity and especially under their combination (Table 2). Furthermore, the stressed plants exhibited a higher de-epoxidation state of the xanthophyll cycle (Table 1), which was well correlated with their J_{NPQ} ($r^2 = 0.81$, $P < 0.001$) levels, as previously described for other woody species (Fusaro *et al*. 2014). The L also contributes to ΔpH-dependent J_{NPQ}, possibly acting on minor monomeric antenna and major trimeric LHCII complexes (Müller *et al*. 2001), as revealed by increases in L levels under stress. These results suggest a precise regulation of the xanthophyll and lutein cycles in *F. rufa* plants in response to stress-induced excess excitation energy, resulting in safe thermal dissipation, especially under combined stress. Regardless, this synchronous positive response is not always observed. For instance, non-regulated thermal dissipation (i.e. $J_{f,D}$) plays an important role in protecting photosynthetic structures from photoinhibition when plants are exposed to salinity alone (Yuan *et al*. 2014). Therefore, it appears that energy dissipation as heat varies based on differences in species, experimental conditions and acclimation states. In fact, regulated thermal dissipation (i.e. J_{NPQ}) not only depends on the xanthophyll and lutein cycles but also includes direct O_2 and oxidised PQ pool quenching as well as triplet-state quenching.

In addition to CO_2 assimilation, the energy allocated to photochemistry (J_{PSII}) can be partially utilised by photorespiration. Photorespiration is considered to protect the photosynthetic apparatus via three functions, whereby the most accepted function is as a potentially important sink of excessive excitation energy (Silva *et al*. 2015). The beneficial effect of photorespiration on photoinhibition has been reported in several plants when subjected individually to mild or moderate drought and salinity, even though different estimation methods, such as low oxygen (2%) and mass spectrometry, were adopted (Abogadallah 2011; Silva *et al*. 2015; Yi *et al*. 2016). Because J_o declined substantially, especially under salinity and combined stress, we conclude that in *F. rufa* plants, photorespiration does not effectively protect the photosynthetic apparatus against photoinhibition. Correspondingly, the J_o/J_c ratio, an important indicator of the relative rate of oxygenation *v.* carboxylation and directly controlled by the kinetic properties of Rubisco (Zhang *et al*. 2015), was reduced under all stress conditions. This response coupled with decreases in J_c/J_{PSII} and P_n further supports the lack of a role for photorespiration in dissipating excess energy under the stresses applied in our study. Hence, it remains a matter of debate whether photorespiration plays an essential function in photoprotection under different stresses, especially under combined stress.

Alternative sinks such as the water-water cycle (i.e. the Mehler-ascorbate peroxidase pathway) can accept electrons from PSII. Several studies have indicated that operation of the water-water cycle at high rates *in vivo* can help plants cope with the excess electrons generated through the photosynthetic transport chain when CO_2 assimilation is restricted by stressful conditions (Hirotsu *et al*. 2004; Yi *et al*. 2016). Nonetheless, the function of the water-water cycle has also been challenged by certain studies showing that the amount of electrons transferred through this pathway is very small (e.g. contributing <5% to linear electron flow in C_3 leaves) and insufficient to protect the photosynthetic apparatus from photoinhibition and damage (Driever and Baker 2011). Notably, our study supports these two views because J_a, which is driven primarily by the water-water cycle, increased under drought and salinity alone but decreased under combined stress, which showed the highest J_a/J_{PSII} (Table 2). Support is also provided by the observed changes in SOD, APX and MDHAR activities (Fig. 4). Furthermore, by optimising the stoichiometry of the ATP/NADPH ratio, the water-water cycle is indispensable for maintaining steady-state rates of CO_2 assimilation and photorespiration (Miyake and Yokota 2000). Accordingly, we speculate that the water-water cycle of *F. rufa* plants is a flexibly protective mechanism that responds to drought and salinity, albeit its function may be limited under these stresses together.

The excessive excitation energy that is neither utilised in photosynthesis nor dissipated by photoprotective mechanisms can inevitably result in overproduction of reactive oxygen

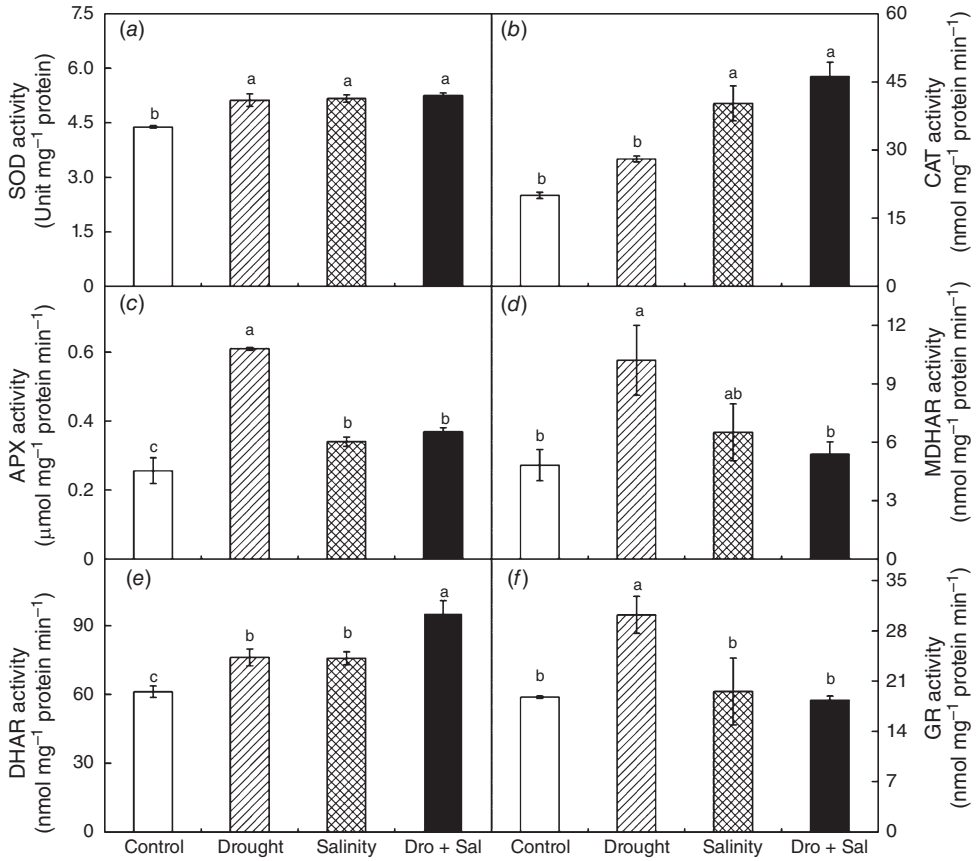

Fig. 4. Activities of antioxidative enzymes in *Fargesia rufa* plants subjected to drought, salinity and their combination. (*a*) Superoxide dismutase (SOD); (*b*) catalase (CAT); (*c*) ascorbate peroxidase (APX); (*d*) monodehydroascorbate reductase (MDHAR); (*e*) dehydroascorbate reductase (DHAR); (*f*) glutathione reductase (GR). Data are the means of four replicates with s.e. shown by vertical bars. Different letters indicate a significant difference at the 5% level.

species (ROS), particularly $O_2^{\bullet-}$ and H_2O_2, in the chloroplasts, mitochondria and peroxisomes. In this study, high $O_2^{\bullet-}$ and H_2O_2 levels were largely produced in leaves of stressed *F. rufa* plants (Fig. 3) and could reflect the degree of oxidative stress. Nonetheless, an obvious increase in H_2O_2 content, especially under salinity and combined stress, was found to be independent of the photorespiration rate, as revealed by a large decrease in J_o (Table 2). This is consistent with a previous report showing that photorespiration is not the main cause of oxidative stress induced by drought and salinity (Abogadallah 2011), even though photorespiration is estimated to generate >70% H_2O_2 in C_3 plants after stress. Moreover, the non-linear relationship between ROS and J_a indicates that the water-water cycle is not the only factor causing oxidative stress because there are other potential sources of ROS. Indeed, due to ROS accumulation, we found that salinity and combined stress were more deleterious to the plasmalemma than was drought, as evidenced by the higher MDA content in the former treatments (Fig. 3). Furthermore, ROS and MDA levels are closely related to the intensity of injury to various organelles, especially chloroplast and mitochondria observed by TEM (Fig. 2), similar to a previous report (Chen *et al*. 2010). It has recently been suggested that damage induced by abiotic stresses is triggered at least in part by oxidative stress (Silva *et al*. 2010).

It is clear that the capacity of the antioxidative enzyme system is highly essential for detoxifying ROS and alleviating oxidative stress. In general, SOD coverts the $O_2^{\bullet-}$ generated by the electron transport chain in the chloroplasts and mitochondria into H_2O_2, and the H_2O_2 produced is then eliminated by CAT, mainly in the peroxisomes, and by the AsA-GSH cycle including APX, MDHAR, DHAR and GR, in all cell compartments. We observed that induction of ROS-scavenging enzyme systems in *F. rufa* plants differs significantly under various stress conditions (Fig. 4). Efficient increases in the activities of SOD and enzymes of the AsA-GSH cycle resulted in limited ROS accumulation, thus providing good protection against oxidative damage under drought alone. Conversely, the activities of AsA-GSH cycle enzymes were overwhelmed by the higher ROS levels under salinity and combined stress, suggesting an insufficient antioxidative capacity to counter the harmful effects of ROS. However, under salinity and combined stress, SOD and CAT activities were enhanced due to stress-induced upregulation of gene expression and/or activation of protein isoforms, which can compensate for relative deficiencies in AsA-GSH cycle enzymes activities. In accordance with previous reports

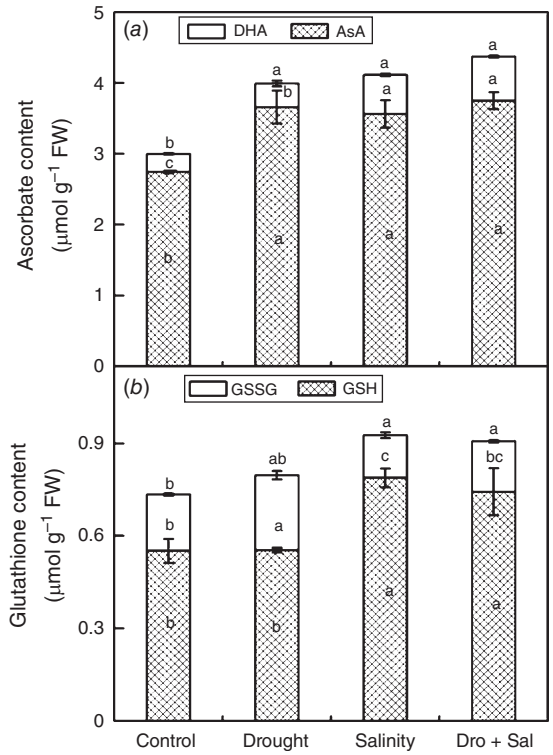

Fig. 5. The contents of ascorbate and glutathione in *Fargesia rufa* plants subjected to drought, salinity and their combination. (*a*) Reduced ascorbate (AsA); oxidised ascorbate (DHA); (*b*) reduced glutathione (GSH); oxidised glutathione (GSSG). Data are the means of four replicates with s.e. shown by vertical bars. Different letters indicate a significant difference at the 5% level.

(Abogadallah 2011; Yi *et al*. 2016), it appears that an enhanced enzyme system did not keep pace with the rate of ROS production because differential regulation of antioxidative enzymes occurred.

Accumulation of non-enzymatic antioxidants such as ascorbate and glutathione not only contributes to substantial reductions in ROS, both directly and indirectly, but also permits fine-tuning of ROS to optimise their functions in cell metabolism (Muscolo *et al*. 2015). The redox states of ascorbate and glutathione are typically modulated by both their rates of synthesis and regeneration, which can be disrupted after stress. In this study, total ascorbate and glutathione contents increased, but the ratios of AsA/DHA and GSH/GSSG remained constant under drought alone (Fig. 5). This suggests that a well-balanced cellular redox state and an optimal function of the AsA-GSH cycle were retained in *F. rufa* plants, and a similar result has been observed in another bamboo species, *Fargesia denudate* (Liu *et al*. 2014). However, based on the low MDHAR activity found, the decrease in the AsA/DHA ratio observed with salinity and combined stress was most likely due to increased AsA biosynthesis rather than recycling capacity (Fig. 4*d*). This finding also suggests that AsA is consumed more rapidly as a substrate for APX activity due to salinity-induced oxidation. In contrast, the high GSH/GSSG ratio in *F. rufa* plants, maintained by increased GSH synthesis and GSSG reduction under salinity and combined stress (Fig. 5), may be indispensable for efficient protection against oxidative damage. This result is in agreement with previous studies demonstrating that glutathione acts as an antioxidant and regulatory signal (e.g. Szalai *et al*. 2009). It is noteworthy that analyses of ascorbate and glutathione at a specific time point only reflect a static condition of the redox balance.

In conclusion, the present study revealed that *F. rufa* plants subjected to drought, salinity and their combination exhibited very different changes in physiological, biochemical and ultrastructural characteristics. Drought was less damaging because the plants had higher thermal dissipation and the water-water cycle capacities, exhibited increases in the activities of SOD/AsA-GSH cycle enzymes, and maintained a favourable redox balance of ascorbate and glutathione. In contrast, salinity and combined stress were more deleterious in terms of inactive photochemistry and further oxidative stress, even though a sporadically protective process such as the redox state of glutathione was activated. Thus, *F. rufa* plants invoke highly efficient protective mechanisms against drought-induced oxidative damage, most likely accelerating recovery of photosynthetic plasticity once the drought stress is relieved. However, an effective mechanism to avoid severe oxidative damage under salinity and combined stress was not observed in this bamboo species. Future studies should focus on *F. rufa* photoprotective and antioxidative responses to oxidative stress at the cellular level under conditions of combined stress.

Acknowledgements

We thank Mr Zongping Tang for help with the fieldwork and Master Lingling Duan for assistance with the laboratory analysis. We also gratefully acknowledge the two anonymous reviewers and the editor for their constructive comments. This work was supported by the National Natural Science Foundation of China (31470621, 31600507) and the Chinese Academy of Sciences 'Light of West China' Program.

References

Abogadallah GM (2011) Differential regulation of photorespiratory gene expression by moderate and severe salt and drought stress in relation to oxidative stress. *Plant Science* **180**, 540–547. doi:10.1016/j.plantsci.2010.12.004

Ahmed IM, Nadira UA, Bibi N, Cao FB, He XY, Zhang GP, Wu FB (2015) Secondary metabolism and antioxidants are involved in the tolerance to drought and salinity, separately and combined, in Tibetan wild barley. *Environmental and Experimental Botany* **111**, 1–12. doi:10.1016/j.envexpbot.2014.10.003

Arrigoni O, Dipierro S, Borraccino G (1981) Ascorbate free radical reductase, a key enzyme of the ascorbic acid system. *FEBS Letters* **125**, 242–244. doi:10.1016/0014-5793(81)80729-6

Cakmak I, Marschner H (1992) Magnesium deficiency and high light intensity enhance activities of superoxide dismutase, ascorbate peroxidase, and glutathione reductase in bean leaves. *Plant Physiology* **98**, 1222–1227. doi:10.1104/pp.98.4.1222

Chaves MM, Oliveira MM (2004) Mechanisms underlying plant resilience to water deficits: prospects for water-saving agriculture. *Journal of Experimental Botany* **55**, 2365–2384. doi:10.1093/jxb/erh269

Chaves MM, Flexas J, Pinheiro C (2009) Photosynthesis under drought and salt stress: regulation mechanisms from whole plant to cell. *Annals of Botany* **103**, 551–560. doi:10.1093/aob/mcn125

Chen LH, Zhang S, Zhao HX, Korpelainen H, Li CY (2010) Sex-related adaptive responses to interaction of drought and salinity in *Populus yunnanensis*. *Plant, Cell & Environment* **33**, 1767–1778. doi:10.1111/j.1365-3040.2010.02182.x

Chen JW, Kuang SB, Long GQ, Yang SC, Meng ZG, Li LG, Chen ZJ, Zhang GH (2016) Photosynthesis, light energy partitioning, and

photoprotection in the shade-demanding species *Panax notoginseng* under high and low level of growth irradiance. *Functional Plant Biology* **43**, 479–491. doi:10.1071/FP15283

Dawalibi V, Monteverdi MC, Moscatello S, Battistelli A, Valentini R (2015) Effect of salt and drought on growth, physiological and biochemical responses of two *Tamarix* species. *iForest-Biogeosciences and Forestry* **8**, 772–779. doi:10.3832/ifor1233-007

Driever SM, Baker NR (2011) The water-water cycle in leaves is not a major alternative electron sink for dissipation of excess excitation energy when CO_2 assimilation is restricted. *Plant, Cell & Environment* **34**, 837–846. doi:10.1111/j.1365-3040.2011.02288.x

Filippou P, Bouchagier P, Skotti E, Fotopoulos V (2014) Proline and reactive oxygen/nitrogen species metabolism is involved in the tolerant response of the invasive plant species *Ailanthus altissima* to drought and salinity. *Environmental and Experimental Botany* **97**, 1–10. doi:10.1016/j.envexpbot.2013.09.010

Flexas J, Bota J, Galmés J, Medrano H, Ribas-Carbó M (2006) Keeping a positive carbon balance under adverse conditions: responses of photosynthesis and respiration to water stress. *Physiologia Plantarum* **127**, 343–352. doi:10.1111/j.1399-3054.2006.00621.x

Foyer CH, Halliwell B (1976) The presence of glutathione and glutathione reductase in chloroplasts: a proposed role in ascorbic acid metabolism. *Planta* **133**, 21–25. doi:10.1007/BF00386001

Fusaro L, Mereu S, Brunetti C, Ferdinando MD, Ferrini F, Manes F, Salvatori E, Marzuoli R, Gerosa G, Tattini M (2014) Photosynthetic performance and biochemical adjustments in two co-occurring Mediterranean evergreens, *Quercus ilex* and *Arbutus unedo*, differing in salt-exclusion ability. *Functional Plant Biology* **41**, 391–400. doi:10.1071/FP13241

Giannopolitis CN, Ries SK (1977) Superoxide dismutases. I. Occurrence in higher plants. *Plant Physiology* **59**, 309–314. doi:10.1104/pp.59.2.309

Hendrickson L, Furbank RT, Chow WS (2004) A simple alternative approach to assessing the fate of absorbed light energy using chlorophyll fluorescence. *Photosynthesis Research* **82**, 73–81. doi:10.1023/B:PRES.0000040446.87305.f4

Hirotsu N, Makino A, Ushio A, Mae T (2004) Changes in the thermal dissipation and the electron flow in the water–water cycle in rice grown under conditions of physiologically low temperature. *Plant & Cell Physiology* **45**, 635–644. doi:10.1093/pcp/pch075

Li YP, Zhang YB, Zhang XL, Korpelainen H, Berninger F, Li CY (2013) Effects of elevated CO_2 and temperature on photosynthesis and leaf traits of an understory dwarf bamboo in subalpine forest zone, China. *Physiologia Plantarum* **148**, 261–272. doi:10.1111/j.1399-3054.2012.01705.x

Liu CG, Wang YJ, Pan KW, Li W, Zhang L, Shen XY, Liu LJ, Deng MR (2014) Responses of the antioxidant defense system to drought stress in the leaves of *Fargesia denudata* seedlings, the staple food of the giant panda. *Russian Journal of Plant Physiology* **61**, 374–383. doi:10.1134/S1021443714020083

Liu CG, Wang YJ, Pan KW, Jin YQ, Li W, Zhang L (2015*a*) Effects of phosphorus application on photosynthetic carbon and nitrogen metabolism, water use efficiency and growth of dwarf bamboo (*Fargesia rufa*) subjected to water deficit. *Plant Physiology and Biochemistry* **96**, 20–28. doi:10.1016/j.plaphy.2015.07.018

Liu CG, Wang YJ, Pan KW, Jin YQ, Liang J, Li W, Zhang L (2015*b*) Photosynthetic carbon and nitrogen metabolism and the relationship between their metabolites and lipid peroxidation in dwarf bamboo (*Fargesia rufa* Yi) during drought and subsequent recovery. *Trees* **29**, 1633–1647. doi:10.1007/s00468-015-1241-0

Miyake C, Yokota A (2000) Determination of the rate of photoreduction of O_2 in the water-water cycle in watermelon leaves and enhancement of the rate by limitation of photosynthesis. *Plant & Cell Physiology* **41**, 335–343. doi:10.1093/pcp/41.3.335

Morari F, Meggio F, Lunardon A, Scudiero E, Forestan C, Farinati S, Varotto S (2015) Time course of biochemical, physiological, and molecular responses to field-mimicked conditions of drought, salinity, and recovery in two maize lines. *Frontiers in Plant Science* **6**, 314. doi:10.3389/fpls.2015.00314

Müller P, Li XP, Niyogi KK (2001) Non-photochemical quenching. A response to excess light energy. *Plant Physiology* **125**, 1558–1566. doi:10.1104/pp.125.4.1558

Munns R (2005) Genes and salt tolerance: bringing them together. *New Phytologist* **167**, 645–663. doi:10.1111/j.1469-8137.2005.01487.x

Muscolo A, Junker A, Klukas C, Weigelt-Fischer K, Riewe D, Altmann T (2015) Phenotypic and metabolic responses to drought and salinity of four contrasting lentil accessions. *Journal of Experimental Botany* **66**, 5467–5480. doi:10.1093/jxb/erv208

Nakano Y, Asada K (1981) Hydrogen peroxide is scavenged by ascorbate-specific peroxidase in spinach chloroplasts. *Plant & Cell Physiology* **22**, 867–880.

Razzaghi F, Jacobsen SE, Jensen CR, Andersen MN (2015) Ionic and photosynthetic homeostasis in quinoa challenged by salinity and drought-mechanisms of tolerance. *Functional Plant Biology* **42**, 136–148. doi:10.1071/FP14132

Scurlock JMO, Dayton DC, Hames B (2000) Bamboo: an overlooked biomass resource? *Biomass and Bioenergy* **19**, 229–244. doi:10.1016/S0961-9534(00)00038-6

Silva EN, Ferreira-Silva SL, Fontenele Ad V, Ribeiro RV, Viégas RA, Silveira JAG (2010) Photosynthetic changes and protective mechanisms against oxidative damage subjected to isolated and combined drought and heat stresses in *Jatropha curcas* plants. *Journal of Plant Physiology* **167**, 1157–1164. doi:10.1016/j.jplph.2010.03.005

Silva EN, Silveira JA, Ribeiro RV, Vieira SA (2015) Photoprotective function of energy dissipation by thermal processes and photorespiratory mechanisms in *Jatropha curcas* plants during different intensities of drought and after recovery. *Environmental and Experimental Botany* **110**, 36–45. doi:10.1016/j.envexpbot.2014.09.008

Suzuki N, Rivero RM, Shulaev V, Blumwald E, Mittler R (2014) Abiotic and biotic stress combinations. *New Phytologist* **203**, 32–43. doi:10.1111/nph.12797

Szalai G, Kellős T, Galiba G, Kocsy G (2009) Glutathione as an antioxidant and regulatory molecule in plants under abiotic stress conditions. *Journal of Plant Growth Regulation* **28**, 66–80. doi:10.1007/s00344-008-9075-2

Thayer SS, Björkman O (1990) Leaf xanthophyll content and composition in sun and shade determined by HPLC. *Photosynthesis Research* **23**, 331–343. doi:10.1007/BF00034864

Tuanmu MN, Viña A, Winkler JA, Li Y, Xu WH, Ouyang ZY, Liu JG (2013) Climate-change impacts on understorey bamboo species and giant pandas in China's Qinling Mountains. *Nature Climate Change* **3**, 249–253. doi:10.1038/nclimate1727

Yen TM, Ji YJ, Lee JS (2010) Estimating biomass production and carbon storage for a fast-growing makino bamboo (*Phyllostachys makinoi*) plant based on the diameter distribution model. *Forest Ecology and Management* **260**, 339–344. doi:10.1016/j.foreco.2010.04.021

Yi XP, Zhang YL, Yao HS, Luo HH, Gou L, Chow WS, Zhang WF (2016) Different strategies of acclimation of photosynthesis, electron transport and antioxidative activity in leaves of two cotton species to water deficit. *Functional Plant Biology* **43**, 448–460.

Yuan YH, Shu S, Li SH, He LZ, Li H, Du NS, Sun J, Guo SR (2014) Effects of exogenous putrescine on chlorophyll fluorescence imaging and heat dissipation capacity in cucumber (*Cucumis sativus* L.) under salt stress. *Journal of Plant Growth Regulation* **33**(4), 798–808. doi:10.1007/s00344-014-9427-z

Zhang Q, Zhang TJ, Chow WS, Xie X, Chen YJ, Peng CL (2015) Photosynthetic characteristics and light energy conversions under different light environments in five tree species occupying dominant status at different stages of subtropical forest succession. *Functional Plant Biology* **42**, 609–619. doi:10.1071/FP14355